Egypt. J. Chem. **Vol. 65,** No. SI: 13B pp. 59 - 72 (2022)

Egyptian Journal of Chemistry

http://ejchem.journals.ekb.eg/

Stratigraphy, Geochemical and Mineralogical Characterization of Lower Miocene Smectitic clay deposits, case: South El-Hammam, Egypt

Dina Othman,[a,*] Ahmed Melegy,[b,*] Ahmed Abdelhalim[a*]

[a]*Department of Geology, Faculty of Science, Cairo University, Giza, Egypt*

b Department of Geological Sciences, National Research Center,Giza,Egypt

Abstract

This work discusses the physical, geochemical and mineralogical characterization of some bentonite resources in South El-Hammam area which are hosted in thick sandstone sequences belonging to the Lower Miocene Moghra Formation. Bentonite samples were characterized by microscopic, SEM, XRD and ICP-MS analyses. Bentonite resources in this study consist of montmorillonite as the main clay mineral of all the analyzed samples. Kaolinite also occurs as minor clay constituents. The identified non-clay minerals include; quartz, albite and calcite. The highest grade of the studied bentonite, contains Si/Al molecular ratio of 2, suggesting absence of detrital quartz. In contrary, the lowest grade of bentonite with alumina content of 15.06%, display Si/Al molecular ratio of 4.34, where free silica dominates over bentonite. The REE content of the Lower Miocene bentonite study area is strongly imparted by LREE signature. The very high CIA index (74.85 and 91.25) suggesting intense chemical weathering of source rock, which is supported by the presence of Ce abnormality, indicating that they were deposited under pluvial conditions.

Keywords: Miocene clay deposits; smectite mineral characterization; CIA index.

1. Introduction

Bentonite is a rock formed of highly colloidal and plastic clays composed mainly of montmorillonite, a clay mineral of the smectite group, and is produced by in situ devitrification of volcanic ash (Shaban et al., 2017). Bentonite possess high cation exchange capacity and absorbs large quantities of water to form thixotropic gels with water. The properties of bentonite are derived from the crystal structure of the smectite group, which is an octahedral alumina sheet between two tetrahedral silica sheets (Faghihian and Godazandeha, 2009). In the study area, South El Hammam area, smectitic clays occur as beds interbedded in the middle part of Lower Miocene Moghra Formation.

The smectitic clay deposits in the northern part of the Western Desert occur in two main localities; South and Southwest Alamein area and South of El-Hammam city. These sediments are considered as a part of the Oligo-Miocene sequence formed in an elongated shallow dipping basin trending E-W and extending over an area of about 115 km long and 65 km width (Abdel-Ghafour et al., 1997 and Abdel-Motelib et al., 2011). In the present work, collaborative petrographical, mineralogical and geochemical techniques have been used to characterize the main genetic and diagenetic events acted on the studied smectitic clay deposits at South El-Hammam area in Egypt (Fig. 1).

2. Geologic setup

In North Western Desert, South El-Hammam area, the smectitic clay deposits are found as beds alternating with Lower Miocene sandstones (Yousf et al., 2018). According to the present field study as well as the reconnaissance survey, the Lower Miocene unit is called Moghra Formation and is composed of fluviomarine sediments which grades northward to more marine facies called Mamura Formation. It consists of clay beds interbedded with clastic sandstone beds. It hosts economically important smectitic clay deposits. The overlying Middle Miocene unit, Marmarica Formation, and is composed mainly of marine fossiliferous carbonates.

In North Western Desert, South El-Hammam area, the studied area of smectitic clay deposits is found between latitudes; 30º 24' 20" and 30º 25' 22" N and longitudes; 29º 14' 15" and 29º 15' 30.77" E (Fig. 1). The studied smectitic clay deposits occur as beds interbedded in the Lower Miocene Moghra Formation. The middle part of Moghra Formation is characterized by the dominance of smectitic clay sediments interbedded with sandstones (Fig 2).

*Corresponding author e-mail: drdinaothman89@yahoo.com ; amelegy@yahoo.com ; aahalim2000@gmail.com.

Receive Date: 05 January 2022, Accept Date: 28 April 2022, First Publish Date: 04 May 2022

DOI: 10.21608/EJCHEM.2022.114695.5217

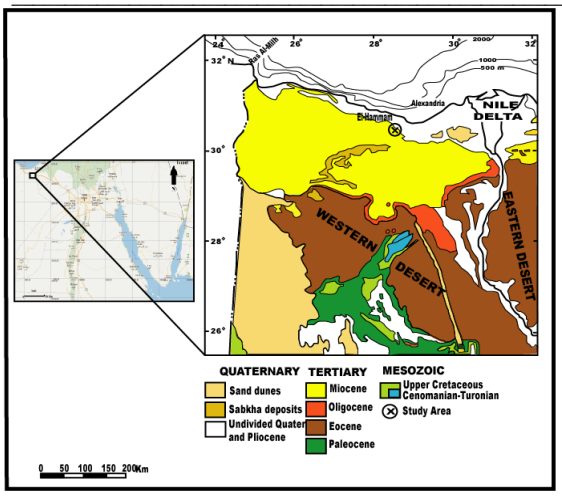

Fig.1. Location and geological map of the smectitic clay study area at North Western-Desert, South El-Hammam City, after Geological Survey of Egypt, 1994

The Lower and Middle Miocene strata, in Egypt, form part of a southward-advancing transgressive system tract (TST). The Early Pliocene sediments represent an abrupt continental transgression following the extreme sea-level and salinity fluctuations of the Upper Miocene. The most recent retreat of the shoreline was marked by Quaternary deposits of the Nile Delta complex. From Upper Eocene to Holocene, magmatic activity was widespread regionally and extensive basaltic and silica-poor volcanic centers formed in the eastern Mediterranean and North Africa. The volcanism reflects the change in the plate tectonic regime induced by Alpine collision, domal uplifts of the basement, and rifting of the Red Sea and Gulf of Suez (Tawadros, 2001).

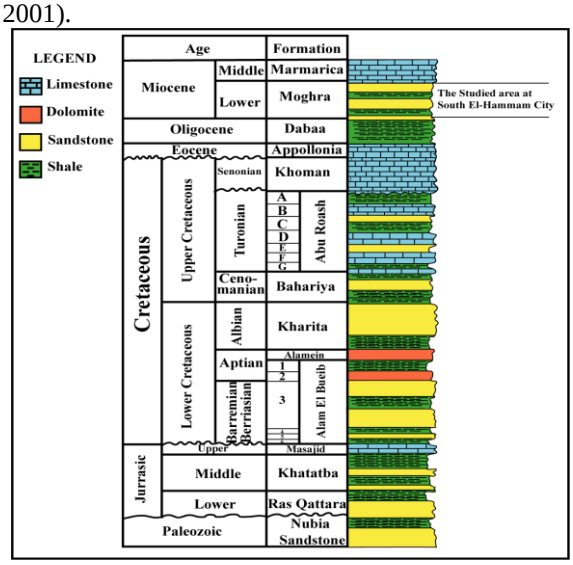

Fig.2. Litholog of South El-Hammam city, North Western Desert showing the smectitic clay bearing formation (Moghra Formation) in the studied area, after El-Nady and Lotfi, 2015.

The smectitic clays are generally found in near shore and fluvial environmental settings rather than in the deep marine. The smectitic clay sequences are underlain and flanked to the east by Mesozoic carbonates, Paleozoic materials, and a Precambrian Basement Complex (Agha et al., 2013). The most frequent origins for the Egyptian smectitic clays are detrital. In North Western desert, south El Hammam area, the smectitic clays of the Late Eocene and Middle Miocene formed from weathered Tertiary basalts at slightly alkaline PHs, while kaolinitic clays formed diagenetically at the expense of smectitic clays (Abu El Ezz et al.,1993).

The smectitic clays in the Northern part of the Western Desert occur in two main localities, south and southwest Alamein area and south of El Hammam city. These sediments are considered a part of an Oligo-Miocene sequence formed in an elongated shallow dipping basin trending E-W and extending over an area about 115 km long and 65 km in width. (Abdel-Ghafour et al., 1997).

South of El-Hammam smectitic clay study area, is located between latitudes; 30º 24' 20" and 30º 25' 22" N and longitudes; 29º 14' 15" and 29º 15' 30.77" E. Based on the field observations south El Hammam smectitic clay deposits is recorded in form of one flat bed extending along the study area with some glauconitic clay inclusions. This smectitic clay bed is about 6.5 m in thickness and is confined to Moghra Formation (Early Miocene).

The following is brief discussion on the stratigraphy of the sedimentary succession in south El Hammam study area. The lateral and vertical variation in facies has been considered during sampling. Based on these field observations, a compiled lithostratigraphic section of these studied areas has been constructed to show the precise location of the collected samples (Fig. 3).

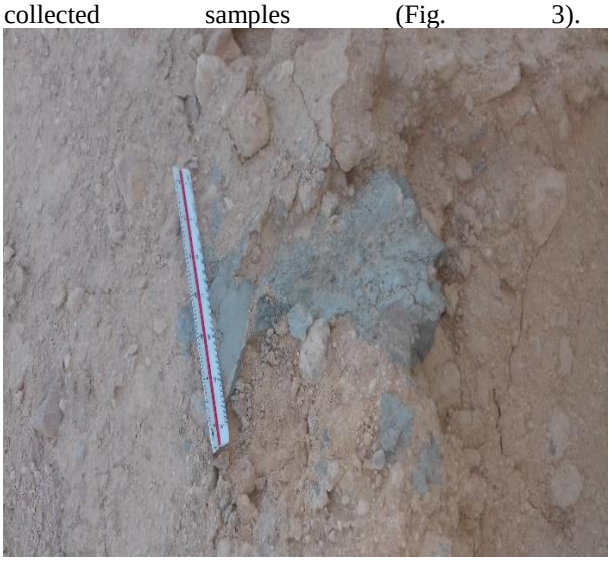

Fig.3. Litholog of South El-Hammam area, North Western Desert, showing the position of smectitic clay bearing Moghra Formation

The Lower Miocene smectitic clay deposits in South El-Hammam city occur within the Moghra Formation (Fig. 4). The smectitic clay lens is overlain by a sandstone bed of 2 m in thickness (Fig. 5). Close to the contact with the overlain sandstone bed, the smectitic clay lens occur (6.5m in thickness). It is of brownish color, soft smectitic clay (Fig. 6). It also shows intercalations of glauconitic clays in the lower part of the lens, the glauconitic clay is green in color and soft (Fig. 7).

Fig.4. Panoramic view of the study area at South El-Hammam City.

Fig.5. Sandstone bed (S.S) overlying smectitic clay lens, at South El-Hammam city.

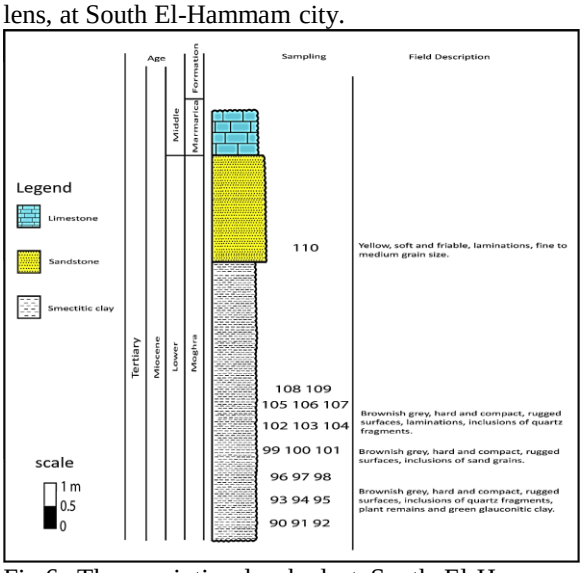

Fig.6. The semiotic clay bed at South El-Hammam city, North Western Desert.

Fig.7. Intercalations of glauconitic clays at the lower part of the smectitic clay lens at South El-Hammam city.

The following is a brief description on the measured and sampled sedimentary section of the smectitic clay-bearing Moghra Formation in South El-Hammam city area, from base to top:

1-Smectitic clay lens (6.5m):

The lower part of the smectitic clay bed is brownish-grey, hard and compact, rugged surfaces, it also contains inclusions of quartz fragments, plant remains and green glauconitic clay.

While the middle part is brownish-grey, hard and compact and contains inclusions of sand grains which is an indication of high silica content.

The upper part of the smectitic clay bed is brownish-grey, hard and compact showing rugged surfaces and laminations, also inclusions of white colored, hard quartz fragments is shown.

2-Sandstone (2 m): Yellow, soft and friable, laminations and of fine to medium grain size.

3. Samples and methods

Twenty-one samples were collected to represent the bentonite lens and their hosting sandstone from the study area. The main petrographical and mineralogical features are studied by petrographic polarizing microscope. Scanning Electron Microscope (SEM), model quanta 250 Field Emission Gun (FEG) attached with Energy Dispersive X-ray (EDX) analyzer, at accelerating voltage 30 kV, was used. The instrument is housed in the Central Laboratories of the Egyptian Mineral Resources Authority (EMRA). The X-ray diffraction analysis was conducted on six whole-rock samples using Cu Kα radiation and Ni filter at scanning rate of 2° (2θ) per minute. The used instrument is housed in the Central Laboratories of the Egyptian Mineral Resources Authority (EMRA) of model; P.W. 1930, at voltage 40 kV and current 30 mA. Since the microscopic examination indicates that the studied bentonite contains about 80%, in average, of clay-size fraction, the X-ray analysis was done on whole-rock samples.

Out of six bulk bentonite samples, one bentonite sample from each layer in the mapped lens was chosen vertically for XRD analysis and four bentonite samples of relatively high grade were chosen for SEM analysis. Twenty samples have been chosen for

chemical analysis of the studied bentonite deposits. These samples represent the lateral and vertical variations of the encountered bentonite lens (Tables 1, 2 and 3). The ratio of alumina/silica and ratios between the common isovalents, such as Zr/Hf, Nb/Ta, Y/Ho and Th/U, are listed in table (4), which involves also the LREE/HREE ratio and ΣREE. The tetrad effect (t1, t3 and t4) of the REE was calculated but it is always of insignificant value.

The chemical analysis of the major, trace and rare earth elements (REE) was conducted on whole rock samples using the inductively coupled plasma-mass spectrometric analysis (ICP-MS) in the Acme lab of Vancouver in Canada (Tables 1, 2 and 3). The obtained data are used to interpret the genetic and diagenetic bearings of the studied kaolin resources.

Results:

The main objective of the SEM examination is to characterize the main microstructures and the diagenetic modifications in four bentonite samples representing the highest grades of the L. Miocene resources. The SEM Petrology Atlas of Welton (1984), with provision of the EDX data, supported the mineral identification. Six bulk bentonite samples, have been chosen for X-ray analysis.

The obtained data indicate that montmorillonite is the main clay mineral of all the analyzed samples. Kaolinite also occurs as minor clay constituents (Figs. 8-13). The identified non-clay minerals include; quartz, albite and calcite.

The intensities and sharpness of montmorillonite have been measured on the basal reflection of montmorillonite in the obtained diffractograms. The obtained data indicate a moderate to well crystalline nature of montmorillonite. In general, the intensity of quartz diffractions increases at the expense of montmorillonite peaks. This observation is also confirmed by microscopic examination where detrital quartz increases at intervals of active terrestrial input to the depositional basin (Figs. 8-13).

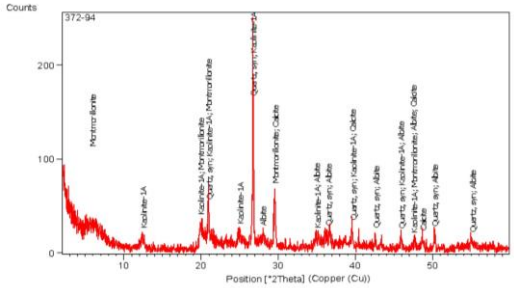

Fig.8.XRD patterns of the brownish-grey bentonite (sample no. 94) collected from Lower Miocene South El-Hammam bentonite deposit.

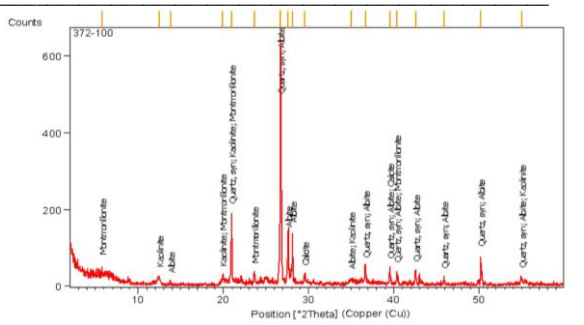

Fig.9. XRD patterns of the brownish-grey bentonite (sample no. 100) collected from Lower Miocene South El-Hammam bentonite deposit

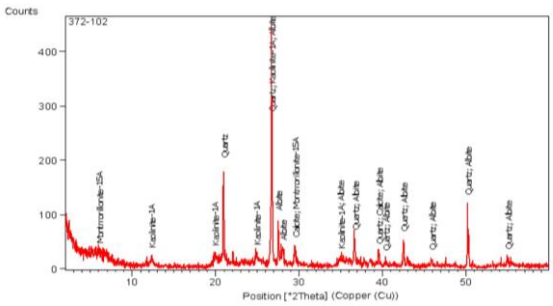

Fig.10. XRD patterns of the brownish-grey bentonite (sample no. 102) collected from Lower Miocene South El-Hammam bentonite deposit

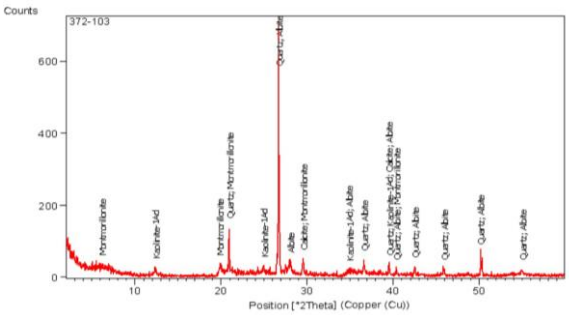

Fig.11. XRD patterns of the brownish-grey bentonite (sample no. 103) collected from Lower Miocene South El-Hammam bentonite deposit

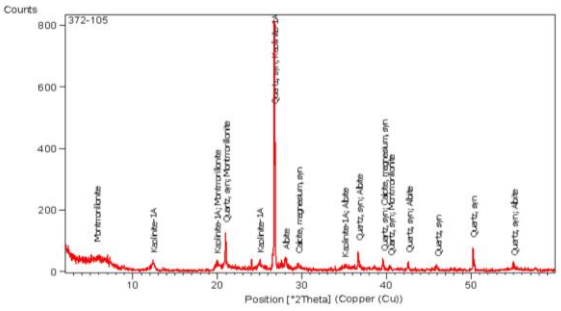

Fig.12. XRD patterns of the brownish-grey bentonite (sample no. 105) collected from Lower Miocene South El-Hammam bentonite deposit

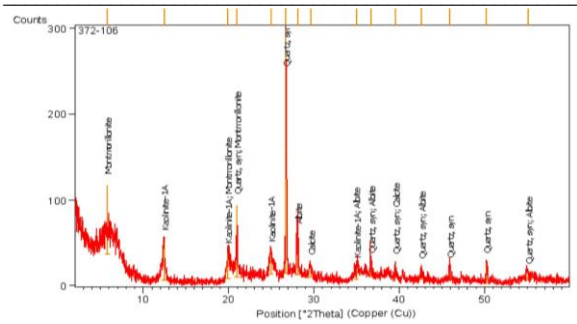

Fig.13. XRD patterns of the brownish-grey bentonite (sample no. 106) collected from Lower Miocene South El-Hammam bentonite deposit

3.1. Discussion

About seven thin and thin-polished sections of bentonite samples collected from the lens under investigation which are representing the smectitic clay mineral lithology were examined. In general, the brownish-grey bentonite bed is dominated by silica. The studied bentonite contains different proportions of organic matter, and dominant clay-size fractions (> 70%, by volume) relative to the detrital quartz grains (13 to 30%). The presence of free silica and organic matter affect the color and compactness of the studied bentonite deposits. The following is short discussion on the main petrographical and mineralogical features of the studied bentonite resource.

The XRD analysis indicates that montmorillonite is quantitatively the main clay mineral constituent of the south El Hammam deposits. However, kaolinite has also been recorded as inconsequential clay constituents (Figs. 8-13). The detected non-clay minerals include quartz in variable concentrations.

Samples from the bentonite lens of South El-Hammam area produces weak reflections related to kaolinite in addition to the major montmorillonite. The intensity of quartz peaks varies considerably from one sample to another. However, based on the obtained XRD and the detailed microscopic examination, it is possible to conclude that the bentonite deposits of South El-Hammam area are enriched in quartz (13-30%).

The megascopic examination suggests that the rock at the bottom of the bentonite lens are brownish-grey with green inclusions of glauconitic clay, however, it is not shown in the XRD analysis and is plastic in nature with the organic matter concentrates along lamination. Going upward, the middle layer in the lens, the bentonite becomes brownish-grey in color with sand grains inclusions. The laminated bentonite with dominant quartz grains occupies the topmost layer of the bentonite lens. The bentonite deposits are frequently dissected by brighter colored veinlets and streaks of chalcedonic-quartz displaying wavy extinction of 1st order interference colors (Figs. 16&17).

Microscopically, the rock is composed of pale brown to brownish grey granules of smectite. It is highly enriched in black and dark brown structurless plant remains. Black colored streaks and lensoidal materials parallel to lamination are also recorded throughout the bentonite lens (Figs. 14-15 -22-23-24). Abundant detrital quartz (up to 30%) of silt to sand sizes are disseminated in the bentonite matrix (Figs. 14-15-16-17-22-23-24). The X-ray analysis indicates that montmorillonite is the main clay mineral with occasional kaolinite, while quartz is the main non-clay mineral with minor presence of albite and calcite.

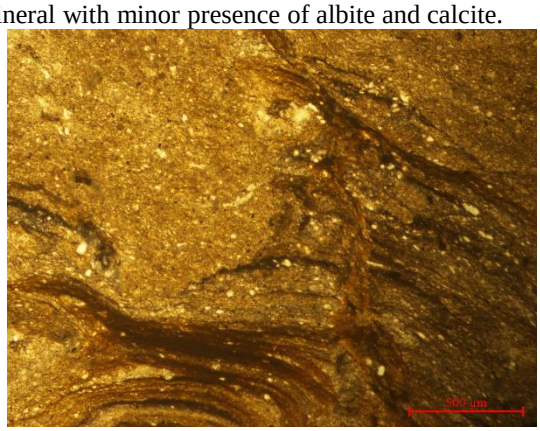

Fig.14. Brownish-grey bentonite (sample 94) showing abundant flaky appearance with preferred orientation. Few fine quartz grains are shown. PPL

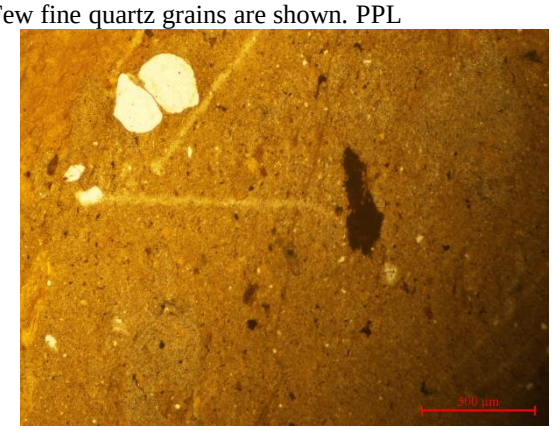

Fig.15. Brownish-grey bentonite (sample 94) containing dark grey plant remains. PPL.

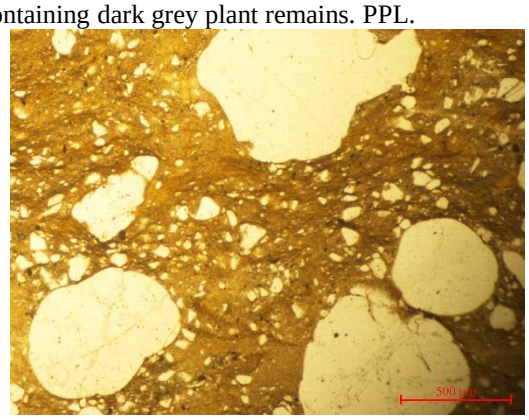

Fig.16. Brownish-grey bentonite (sample 100) showing rounded quartz granule in a brown silty bentonite matrix. PPL.

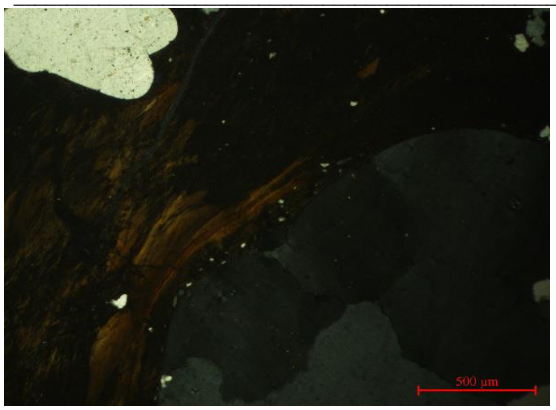

Fig.17. Brownish-grey bentonite (sample 100) showing rounded quartz granule in a brown silty bentonite matrix. CN.

Scanning Electron images of South El-Hammam area, lower part of the lens (sample number 94 and 100) show petals-like structure of smectite, smooth surfaces of smectite along with poor to medium crystallinity (Figs. 18 and 19).

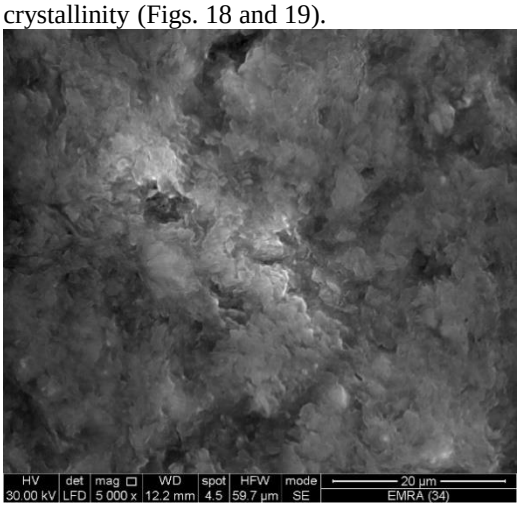

Fig.18. BSE image of bentonite of the lower part of the lens, sample 94, at South El-Hammam area, showing petals-like structure of smectite.

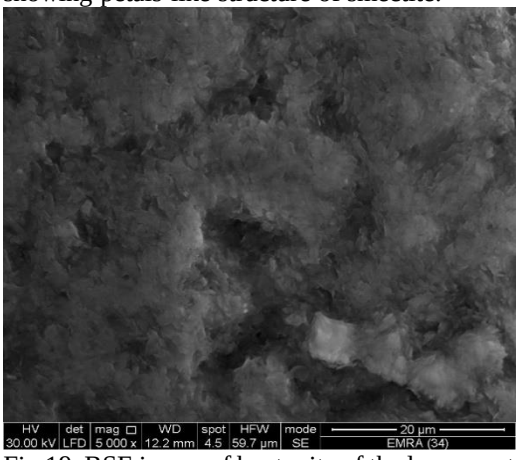

Fig.19. BSE image of bentonite of the lower part of the lens, sample 100, at South El-Hammam area, showing petals-like structure of smectite.

The SEM examination of such masses showed that the shape of bentonite is smoothed surfaces and proposes their organic composition (Figs. 18 & 19). The obtained EDX data suggest organic composition of such masses, where C appears as major component with the bentonite ingredients as represented by Al, Si, Na, Ca and Mg. Iron is not detected in the analysis (Figs. 20 & 21).

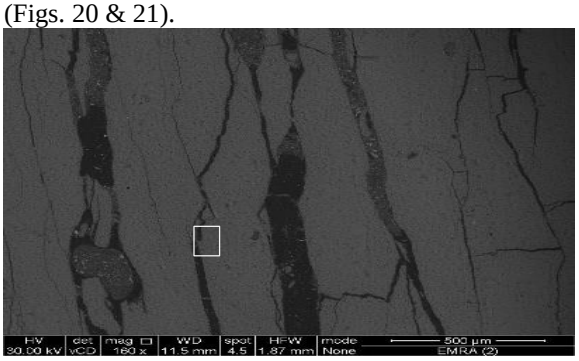

Fig.20. BSE image of dark brown plant remains appearing in Fig. 3.22, of brownish dark grey organic mass embedded within bentonite matrix. Sample 94 in South El-Hammam area

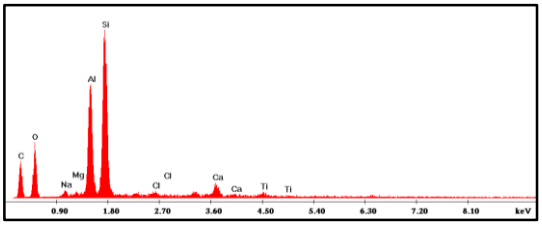

Fig.21. EDX spectrum of the organic-rich mass.

Measuring the sharpness of montmorillonite, based on the width of its basal reflection at its mid-height, indicates a moderate to a well crystalline nature. The presence of well-defined sharp and clearly resolved peaks of montmorillonite support the deduced moderate-well crystallinity of the examined South El-Hammam bentonite.

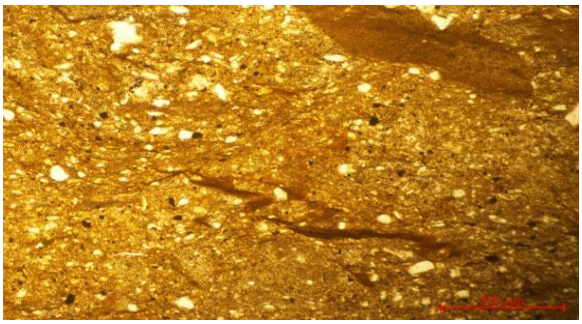

Fig.22. Bentonite sample 102 at the middle part of the bentonite lens showing brown structurless bentonite bodies and organic-rich flakes can be seen at the lower and upper right side of the microphotograph, PPL.

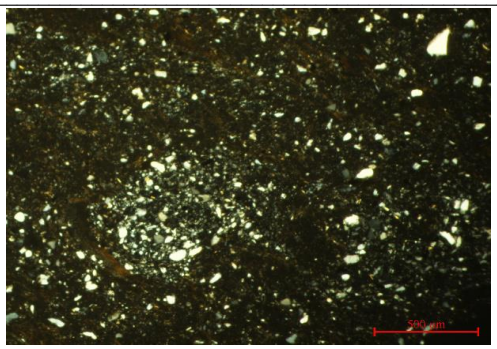

Fig.23.Subangular quartz fragment embedded in the sandy bentonite matrix. CN

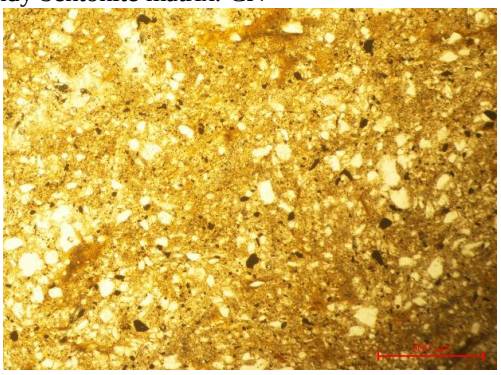

Fig.24. Brownish-grey upper part of the bentonite lens at South El-Hammam area. The organic matter and quartz fragments are also shown scattered in the bentonite matrix, PPL.

The SEM examination confirms the poor edges and outlines of petals shape of the smectite composing the middle and upper parts of bentonite lens (Figs. 25 and 26).

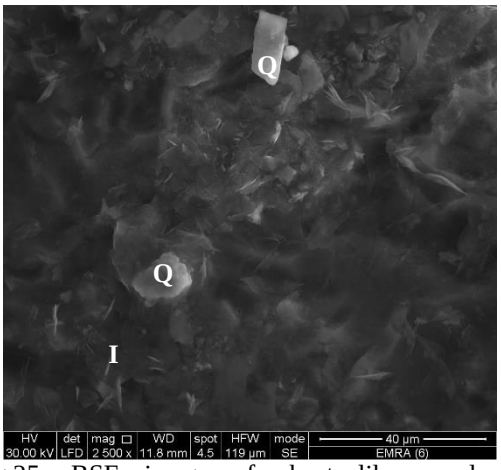

Fig.25. BSE image of sheet like, moderately crystalline sheet-like smectite and scattered quartz (Q) fragments and needle-like crystals of illite (I), sample 102. Brownish-grey bentonite of the upper part of bentonite lens of South El-Hammam area.

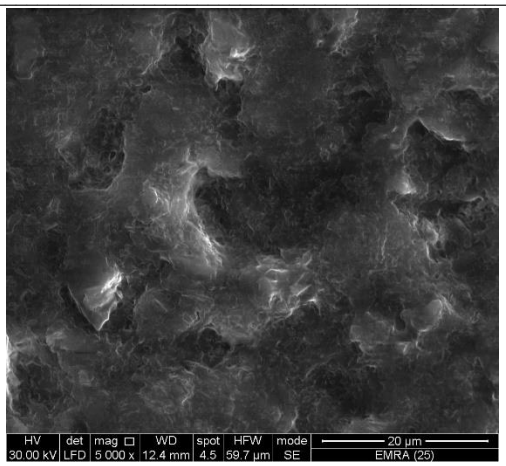

Fig.26. BSE image of sheet like, moderately crystalline petals- like smectite, sample 105. Brownish-grey bentonite of the upper part of bentonite lens of South El-Hammam area.

4. Geochemistry of smectitic clay deposits

The present work discusses the diagnostic geochemical characteristics of the Lower Miocene sedimentary kaolin deposits under consideration. The Lower Miocene bentonite deposits are alternated with the sandstones of the Moghra Formation.

4.1 Materials and methods

Twenty samples have been chosen for chemical analysis of the studied bentonite deposits. These samples represent the lateral and vertical variations of the encountered bentonite lense. The ratio of alumina/silica and ratios between the common isovalents, such as Zr/Hf, Nb/Ta, Y/Ho and Th/U, are listed in table (1), which involves also the LREE/HREE ratio and ΣREE. The tetrad effect (t1, t3 and t4) of the REE was calculated but it is always of insignificant value.

The chemical analysis of the major, trace and rare earth elements (REE) was conducted on whole rock samples using the inductively coupled plasma-mass spectrometric analysis (ICP-MS) in the Acme lab of Vancouver in Canada (Tables 1-4). The obtained data are used to interpret the genetic and diagenetic bearings of the studied bentonite resources.

5. Results and discussion

Based on color South El-Hammam bentonite resources are generally brownish in color. The coloring agents are organic matter, which renders the bentonite dark shades, and ferruginous materials which gives it the brownish shades. The organic matter can be destructed upon heating whereas the ferruginous material is costly to eliminate. Petrographically, the ferruginous coloring agents concentrate along lamination but may also stain the resources.

The averages of the obtained results on South El-Hammam bentonite resources are compared with published data on domestic and world-wide deposits, as well as with the Upper Continental Crust as well (Table 5).

The obtained data reflect a marked difference in composition between the different occurrences or even along the smectitic clay sedimentary sequence in the same area. The comparison between smectitic clay from the studied area and upper continental crust (Rundnick and Gao, 2010) shale resources proposes that South El-Hammam bentonite deposits is considerably enriched in Al2O3, TiO2 and iron oxides while it is depleted in alkalis (Na2O and K2O), CaO and MgO (Fig. 27). This probably reflects less availability of dolomite and calcitic material in the study area of bentonite resources, while the enrichment in Al2O3 reflects a higher economic grade of the bentonite deposits. The enrichment in Fe2O3 content probably indicates more availability of hematite and goethite minerals available in South El-Hammam bentonite resources.

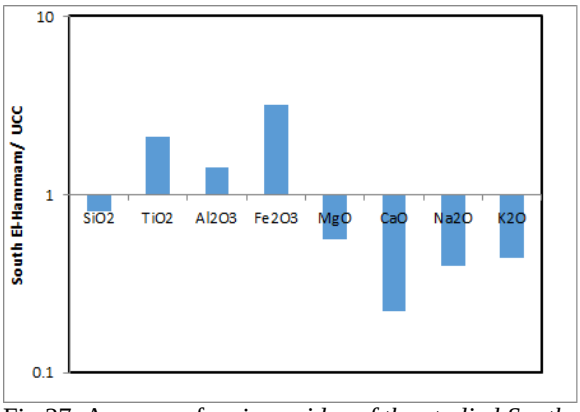

Fig.27. Average of major *oxides of the studied South El-Hammam bentonite deposits normalized to upper continental crust (UCC) (Rundnick and Gao, 2010)*

Table 1 :Chemical analysis data of major oxides (Wt. %) of the studied bentonite

Locality	Sample	SiO_2	TiO_2	Al_2O_3	Fe_2O_3	MgO	CaO	Na_2O	K_2O	P_2O_5	L.O.I	Total
South El-Hammam	90	51.96	1.55	22.65	8.85	1.73	0.59	1.31	1.23	0.09	9.99	99.95
	91	49.31	1.24	23.79	9.66	0.73	1.29	1.46	0.9	0.5	10.2	99.08
	92	51.2	0.99	23.13	9.26	1.24	0.79	1.1	1.3	0.05	10.6	99.66
	93	48.52	1.86	25.18	9.64	1.36	0.47	1.28	1	0.11	10.5	99.92
	94	55.39	1.1	20.87	9.04	1.68	0.54	1.3	1.37	0.26	8.4	99.95
	95	55.31	1.09	20.84	9.89	1.72	0.16	1.55	1.43	0.29	7.69	99.97
	96	56.37	1.34	21.99	7.08	1.15	0.8	0.84	1.45	0.09	8.6	99.71
	97	52.76	1.19	25.99	6.07	0.97	0.45	0.78	1.26	0.09	10.4	99.96
	98	53.22	1.53	23.07	7.34	1.74	0.59	1.35	1.42	0.06	9.59	99.91
	99	60.44	1.57	18.2	7.35	1.88	0.47	1.5	1.24	0.03	7.3	99.98
	100	65.41	1	15.06	5.72	1.43	2.08	1.38	1.6	0.09	6.02	99.79
	101	50.85	2	24.46	8.34	1.3	0.44	1.21	0.99	0.12	10.2	99.91
	102	50.35	1.66	25.57	7.34	1.42	1.06	1.32	0.94	0.44	9.88	99.98
	103	54.01	1.51	20.89	8.18	1.86	0.58	2.19	1.31	0.11	9.29	99.93
	104	52.14	1.53	24.48	7.11	1.73	0.45	1.37	1.21	0.04	9.91	99.97
	105	53.9	1.14	20.93	8.7	1.28	1	1.66	1.17	0.08	10.1	99.96
	106	60.6	1.14	18.06	7.29	1.42	0.37	1.1	1.41	0.13	8.11	99.63
	107	59.62	1.35	20.39	5.81	1.08	0.89	1.22	1.57	0.06	8	99.99
	108	52.82	1.22	21.81	7.77	1.18	2.44	1.12	1.41	0.11	10.1	99.98
	109	50.11	1.23	24.56	8.21	0.9	0.7	1.47	0.95	0.07	11.68	99.88

Table 2: Chemical analysis data of trace elements (ppm) of the studied bentonite

Locality	Sample	Be	Cs	Rb	Sr	V	Co	Sn	Ga	W	Zr	Hf	Nb	Ta	Th	U
South El-Hammam	90	3	<0.1	47	389	177	29	7	14.5	4	210	6	14	0.8	12.6	3.4
	91	2	<0.1	47	158	128	12	5	13.5	3.3	223	6.2	32	1.8	18	4
	92	1	<0.1	39	284	200	15	10	11.9	4.1	360	9.9	29	1.7	23	5.7
	93	1	<0.1	48	217	209	20	8	11.8	4.1	324	9.1	26	1.5	20	3.8
	94	2	0.2	55	182	182	17	3	9.8	2.7	318	9	37	2.1	17.6	4.2
	95	3	0.4	53	199	183	21	5	14.6	3	218	6.2	30	1.7	21	5
	96	<1	0.2	56	162	182	22	3	11.5	3.1	294	8.2	30	1.6	14.6	3.6
	97	2	0.1	52	125	180	30	4	10.1	3	217	6	26	1.5	17.3	4
	98	3	<0.1	33	102	177	29	5	16.6	3.4	229	6.2	26	1.5	13	2
	99	3	<0.1	29	155	128	12	5	18.8	2.4	301	8.5	46	2.7	18.5	4.6
	100	2	<0.1	38	108	200	15	4	15.5	2.3	338	9.8	19	1.1	18.2	4.2
	101	1	<0.1	32	108	209	20	3	17.2	3.4	400	11	21	1.2	23	7

	102	4	0.2	38	148	179	17	4	12.8	2.9	354	9.8	23	1.3	21.5	5
	103	1	0.1	37	104	195	19	4	17.2	2.9	232	6.3	26	1.5	21	6
	104	2	0.2	34	99	182	22	3	12.8	2.8	234	6.3	25	1.4	17.7	4.3
	105	3	0.4	36	98	180	30	5	17.2	3.1	237	6.5	32	1.8	21.6	5
	106	<1	0.2	38	108	193	13	3	10.3	3.2	308	8.2	33	1.9	13	3
	107	2	0.1	37	118	183	20	3	9.9	3.1	293	7.9	24	1.4	21	5.6
	108	3	<0.1	38	127	175	22	5	12.9	3.5	258	7.2	34	1.8	12	2.1
	109	4	<0.1	37	118	178	23	5	13	2.5	348	9.8	28	1.6	11	2

Table 3: Chemical analysis data of the rare earth elements of the studied bentonite

Locality	Sample	Y	La	Ce	Pr	Nd	Sm	Eu	Gd	Tb	Dy	Ho	Er	Tm	Yb	Lu
South El-Hammam	90	21	52.4	58.4	10.22	26.2	5.94	0.97	5.48	1.1	7.73	0.74	4.09	0.71	4.22	0.72
	91	22	26.9	69.4	7.94	22	6.04	1.45	5.65	0.58	3.88	0.78	2.54	0.5	2.46	0.49
	92	41	50.1	45.5	11.47	25.8	10.38	2.47	9.65	1.39	8.08	1.46	3.87	0.71	3.7	0.7
	94	18	27.7	98.4	6.67	11	2.88	1.27	5.88	1.29	8.07	0.64	5.1	1.19	5.31	1.01
	95	21	27	78.45	6.66	10.2	4.25	1.25	5.6	1.19	8..04	0.75	5	0.83	5.21	0.8
	96	26	72.9	100.2	16.52	27.2	7.95	1.76	7.65	1.23	7.3	0.92	3.8	0.68	3.94	0.67
	97	40	79.6	78.4	19.45	51.4	12.54	2.79	9.65	1.41	7.94	1.42	3.6	0.7	3.66	0.71
	98	22	54.7	95.2	11.88	33.6	6.95	1.72	6.54	1.21	7.24	0.78	3.7	0.68	3.69	0.68
	99	18	52.5	102.5	10.51	26.5	6.02	1.53	5.85	1.2	7.84	0.64	4.31	0.81	4.64	0.78
	100	25	77	75.6	19.84	59	15.29	3.44	13.65	2.1	11.49	0.89	7.62	0.8	5.16	0.88
	101	24	52.4	77.68	10.45	26.1	6.1	1.43	5.2	1.19	7.81	0.85	4.3	0.82	4.7	0.79
	102	22	86.6	66.4	19.35	30.4	8.75	1.88	6.98	1.17	7.8	0.78	3.74	0.65	3.47	0.68
	103	49	51.5	100.3	10.37	24.1	5.36	1.3	5.32	1.01	6.17	1.5	3.2	0.62	3.47	0.66
	104	23	73.3	98.8	15.47	36.4	8.57	2.11	8.12	1.28	7.08	0.82	4.2	0.68	3.21	0.63
	105	20	50.1	57.35	12.45	39.3	8.58	2.24	8.5	1.29	7.81	0.71	4.3	0.73	4.16	0.7
	106	24	74.3	75.4	15.57	46.5	8.65	2	7.25	1.26	7.1	0.84	4.2	0.67	3.19	0.66
	107	22	79.2	89.5	19.52	51.5	12.54	2.59	9.2	1.38	7.73	0.78	3.7	0.69	3.72	0.69
	108	23	72.3	80.5	16.74	37.5	7.81	1.7	7.52	1.22	7.2	0.82	3.87	0.69	3.99	0.69

Table 4:Important ratios of alumina/silica, common isovalents and total REE in the studied bentonite

Locality	Sample No.	Al_2O_3/ SiO_2	Zr/Hf	Nb/Ta	Y/Ho	Th/U	LREE/ HREE	Total REE
South El-Hammam	90	0.4	35	17.5	28.37	3.7	5.94	178.92
	91	0.5	35.96	17.77	28.2	4.5	7.21	150.61
	92	0.4	36.36	17.05	28.08	4	4.47	175.28
	93	0.5	35.6	17.33	28.26	5.26	10.16	278.75
	94	0.4	35.33	17.61	28.12	4.19	4.93	176.41
	95	0.4	35.16	17.64	28	4.2	4.41	155.23
	96	0.4	35.85	18.75	28.26	4	8.04	252.72
	97	0.5	36.16	17.33	28.16	4.32	7.57	273.27
	98	0.4	36.93	17.33	28.2	6.5	7.71	228.57
	99	0.3	35.41	17.03	28.12	4	7.17	225.63
	100	0.2	34.48	17.27	28.08	4.33	5.36	292.76
	101	0.5	36.36	17.5	28.23	3.28	6.38	199.82
	102	0.5	36.12	17.69	28.2	4.3	7.79	238.65
	103	0.4	36.82	17.33	28.16	3.5	8.24	214.88
	104	0.5	37.14	17.85	28.04	4.11	8.27	260.67
	105	0.4	36.46	17.77	28.16	4.32	5.51	198.22
	106	0.3	37.56	17.36	28.57	4.33	8.11	247.59
	107	0.3	37.08	17.14	28.2	3.75	8.28	282.74
	108	0.4	35.83	18.88	28.04	5.7	7.76	242.55
	109	0.5	35.51	17.5	28.33	5.5	5.69	202.63

Table 5: Averages of the preset work compared with published data and Upper Continental Crust

Oxides% or Elements	Present Work	Fayoum Bentonite	G.Hamza Bentonite	Upper Continental Crust (UCC)

NA*: Not analysed

ppm	South El-Hammam (n=20)	Abayazeed (2012)	Abayazeed (2012)	Ekosse (2001)	Rundnick & Gao (2010)
SiO_2	54.21	57.31	51.95	45.34	66.60
TiO_2	1.36	1.19	1.53	0.68	0.64
Al_2O_3	22.09	20.66	22.79	28.57	15.40
Fe_2O_3	7.93	7.35	8.69	2.65	5.04
MgO	1.394	1.34	1.44	1.06	2.48
CaO	0.8	1.01	0.75	0.08	3.59
Na_2O	1.32	1.18	1.38	0.23	3.27
K_2O	1.25	1.45	1.17	3.87	2.80
P_2O_5	0.14	0.16	0.18	0.06	0.15
L.O.I	9.32	8.54	9.30	12.28	NA
Rb	41.2	52	38	119	84
Sr	155.45	217	121	136	320
V	181	182	219	229	97
Co	20.4	23	23	50	17.3
Ga	13.59	NA*	NA*	NA	17.5
Zr	284.8	273	299	240	193
Hf	7.9	NA*	NA*	NA	5.3
Nb	28.05	NA*	NA*	17	12
Ta	1.59	NA*	NA*	NA	0.9
Th	17.78	NA*	NA*	14	10.5
U	4.22	NA*	NA*	NA	2.7
Y	24.55	NA*	NA*	22	21
∑REE	223.8	NA*	NA*	NA	148

The comparison with respect to trace elements shows depletion of South El-Hammam bentonite deposits in Rb, which can be considered as a direct feedback for the marked decrease in K2O. South El-Hammam bentonite deposits are also enriched in V, Co, Zr, Hf, Nb, Ta, Th, U, Y and REE but depleted in Sr and slightly depleted in Ga (Fig. 28).

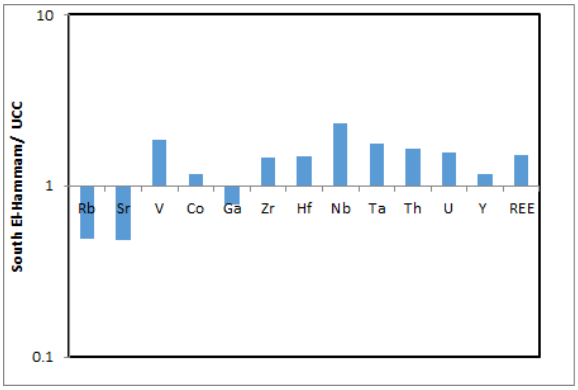

Fig.28. Trace elements average of the studied South El-Hammam bentonite deposits normalized to upper continental crust (UCC) (Rundnick and Gao, 2010)

The comparison between the bentonite deposits of the study area with those Gabal Hamza (Abayazeed, 2012) indicates relative enrichment in silica at the expenses of alumina, while compared to El-Fayoum deposits (Abayazeed, 2012) indicates enrichement of alumina as a direct feedback of increasing the alumina content which means that the bentonite deposits of the study area is of higher grade than that of El-Fayoum bentonite deposits and slightly less in grade than those of Gabal Hamza, except for samples 91,92,93, 97, 98, 101,102, 104 and 109 which have higher alumina content (23.13%-25.99%) than those of Gabal Hamza deposits (22.79%).

Bentonite versus quartz:

From petrographic point of view, the studied bentonite deposits of South El-Hammam area are enriched in detrital quartz of medium and large sizes. However, the negative relationship between alumina and silica indicates that free-silica, that occurred due to discrepancy in the paleo-currents and also subaerial and weathering activities, seems to be the main diluting agent of bentonite grade (Fig. 29).

Sample number 97 (middle part of the bentonite lens), which represents the highest grade of the studied bentonite, contains Si/Al molecular ratio of 2, suggesting absence of detrital quartz. In contrary, sample number 100 (upper part of the bentonite lens), the least grade of bentonite with alumina content of

15.06%, display Si/Al molecular ratio of 4.34, where free silica dominates over bentonite.

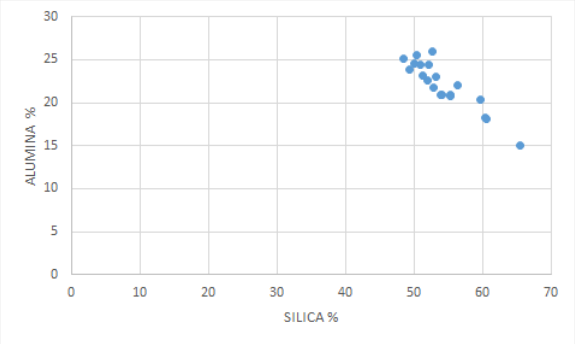

Fig.29. Opposite relationship between silica and alumina of the studied bentonite.

Chemical weathering Index:

Chemical index of alteration (CIA) is the most reliable index for measuring intensity of weathering in the sedimentary environments. It was proposed by Nesbitt and Young (1982), according to the equation; CIA=(Al2O3/Al2O3+Na2O+K2O+CaO)*100 assuming that chemical weathering leads to mobilization of alkalis and CaO from silicate minerals relative to the immobile alumina. According to Fedo et al., (1995), the CaO in the above equation represents only CaO in the feldspar lattice and not that in carbonate phases. The studied bentonite deposits display CIA values ranging between 74.85 and 91.25, suggesting intense chemical weathering of source rock (Fig. 30).

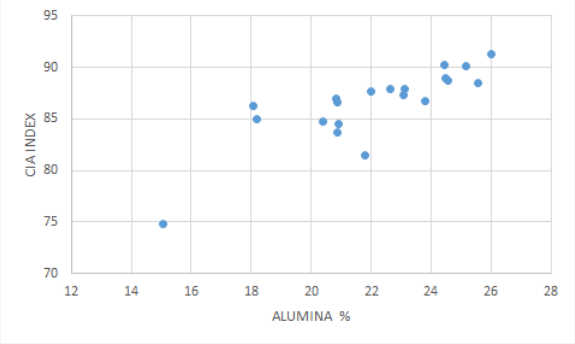

Fig.30. Relationship between CIA and alumina as a measure of bentonite grade

The above diagram shows that the grade of the bentonite deposits which increases with increasing the CIA index. The relation of magnesia versus potash plots the bentonite deposits concentrate in the high magnesia and high potash field, which might be due to the presence of illite and chlorite materials (Fig. 31).

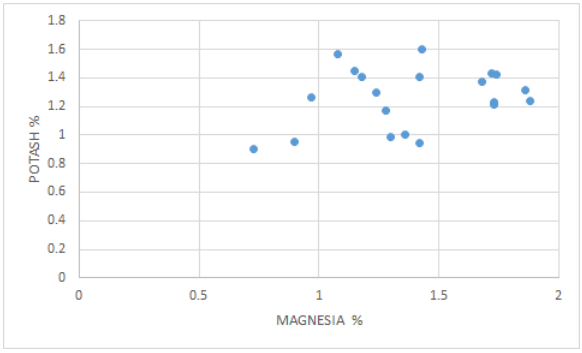

Fig.31. Magnesia versus potash relation showing the high magnesia, high potash field of all samples of bentonite deposits of the study areas

Trace elements:

The present discussion on the trace elements is based on data of 15 trace elements in the studied whole bentonite deposits (Table 2). These trace elements include alkalis (Rb and Cs), alkali earths (Be and Sr), heavy metals (V, Co and Sn), high field strength elements (Zr, Hf, Nb, Ta and W), and radionuclides (Th and U).

The comparison between the bentonite deposits of study areas points to the marked deficiency in Rb, as an immediate response to the low K2O, as well as marked deficiency in Sr in addition to slight deficiency in Ga. South El-Hammam deposits are markedly enriched in Nb, Ta, V, Zr, Hf, Y and REE, accompanied with slight enhancement of Y and Co (Fig. 32). Abayazeed (2012) recorded average concentration of Zr (299 ppm) for Gabal Hamza bentonite deposits and Zr (273 ppm) as average for bentonite deposits of El-Fayoum area.

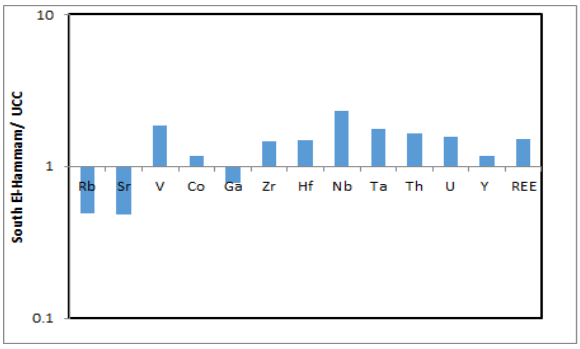

Fig.32. Average trace elements composition of South El-Hammam bentonite normalized to that of the UCC

According to Weyer, et al., (2002) the most precise chondritic ratios for Zr/Hf and Nb/Ta are 34.2 ± 0.3 and 17.6 ± 1, respectively. The latter geochemical pair (i.e., Nb/Ta) seems to be very consistent (17.5, in average) with the chondritic one (Fig. 33). Although the relationship between Zr and its heavier isovalent (Hf) is very strong, there is coherence between the bentonite deposits in the study areas. The average Zr/Hf ratio for the study areas is 36 (Fig. 34). Providing that both Zr and Hf are partners of zircon,

which is the detrital mineral proper, the high Zr/Hf ratio may reflect derivation from more differentiated provenance (e.g., basalt)

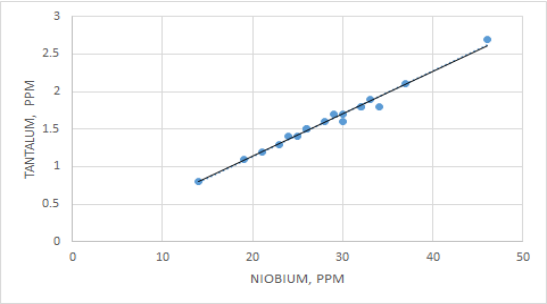

Fig. 33. Perfect coherence between Nb and Ta in the studied bentonite deposits

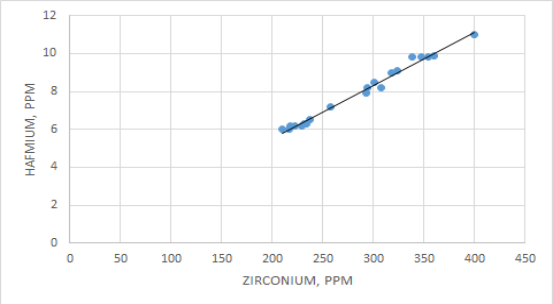

Fig. 34. Perfect coherence between Zr and Hf in the studied bentonite deposits

The Y/Ho ratio is close to the chondritic value (28) for all the analyzed samples. In contrary, the Th/U ratio reflects distinct differentiation and common state of disequilibrium. In all cases, Th content (11 to 23 ppm) predominates over that of U (2 to 7 ppm). The Th/U ratio is always non-CHARAC (charge and radius control), where it varies between 3.3 and 6.5 for the study areas bentonite deposits (Fig. 35).

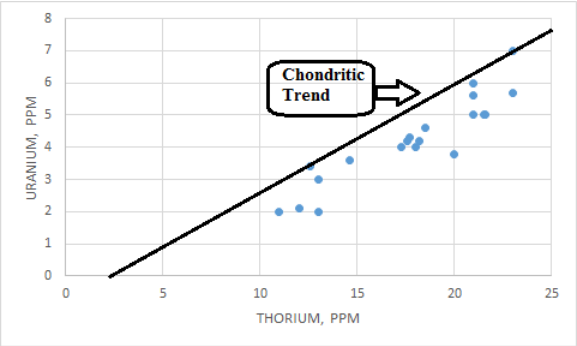

Fig. 35. Plot of thorium versus uranium, showing the non-CHARAC behavior of the studied bentonite deposits

The TH/U ratio for most of the bentonite samples being below the chondritic (CHARAC) value (2.8) suggests mobilization out of U from the bentonite resources. Under the prevailing exogenic environments, U oxidizes into its hexavalent mobile state while Th remains in the tetravalent immobile state. Bentonite samples of the study areas show marked loss of U relative to Th. The mobilization of U must had taken place during the pluvial periods.

Rare earth elements (REE) geochemistry:

The ΣREE content ranges between 150 and 292 ppm, averaging 223.79 ppm for South El-Hammam bentonite deposits. The obtained REE budget is much higher, generally, comparable to the values quoted, for the Upper continental crust as reported by Rudnick and Gao (2010) (148 ppm). The REE budget of the bentonite study area shows intimate coherence (Fig. 36). The straightforward explanation of such discrepancies is that the REE content of the bentonite study area is strongly imparted by LREE signature.

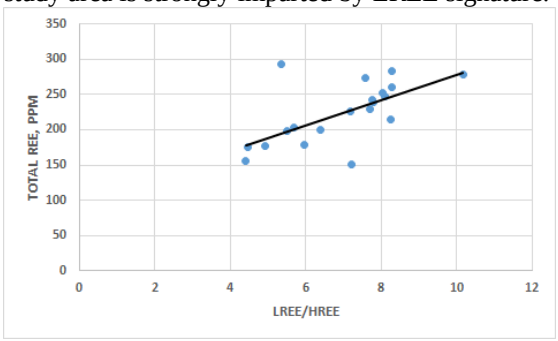

Fig. 36. Relationship between total REE content and LREE/HREE for the studied bentonite resources

Normalized REE patterns:

The REE contents of the studied bentonite resources have be normalized to chondrite and North American Shale Composite (NASC) as quoted by McLennan, (1989) and Gromet, et al. (1984), respectively. The normalization to chondrite (Fig. 37) reflects the following important inferences;

1. LREE have wider variation than HREE for the study areas of bentonite.
2. Eu negative anomaly in the studied bentonite samples.
3. The analyzed bentonite deposits displays Ce abnormality, which indicates that they were deposited under pluvial conditions.
4. The slope of the patterns reflects higher predominance of the LREE over the HREE for the studied bentonite.

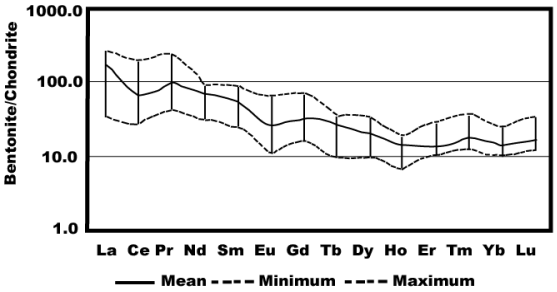

Fig. 37. Chondrite-normalized REE patterns of the studied bentonite resources

6. Conclusions

Bentonite deposits in South El-Hammam City represented one of the most important reserve that would be used in traditional and modern industrial purposes.

The XRD analysis of the studied bentonite suggests that montmorillonite is the main constituent and is sometimes associated with subsidiary kaolinite. The most dominant non-clay mineral is quartz, besides minor albite and calcite. The intensities and sharpness of montmorillonite have been measured on the basal reflection of montmorillonite in the obtained diffractograms. The obtained data indicate a moderate to well crystalline nature of montmorillonite. In general, the intensity of quartz diffractions increases at the expense of montmorillonite peaks. This observation is also confirmed by microscopic examination where detrital quartz increases at intervals of active terrestrial input to the depositional basin.

Moreover, the highest grade of the studied bentonite, contains Si/Al molecular ratio of 2, suggesting absence of detrital quartz. In contrary, the lowest grade of bentonite with alumina content of 15.06%, display Si/Al molecular ratio of 4.34, where free silica dominates over bentonite. The comparison with respect to trace elements shows depletion of South El-Hammam bentonite deposits in Rb, which can be considered as a direct feedback for the marked decrease in K2O. South El-Hammam bentonite deposits are also enriched in V, Co, Zr, Hf, Nb, Ta, Th, U, Y and REE but depleted in Sr and slightly depleted in Ga. The Lower Miocene bentonite is characterized by a higher contribution of LREE. The TH/U ratio for most of the bentonite samples being below the chondritic (CHARAC) value (2.8) suggests mobilization out of U from the bentonite resources. Under the prevailing exogenic environments, U oxidizes into its hexavalent mobile state while Th remains in the tetravalent immobile state. Bentonite samples of the study areas show marked loss of U relative to Th. The mobilization of U must had taken place during the pluvial periods. The very high CIA index (74.85 and 91.25), suggesting extensive limits of chemical weathering, supported by the analyzed bentonite deposits displays Ce abnormality.

The ΣREE content ranges between 150 and 292 ppm, averaging 223.79 ppm for South El-Hammam bentonite deposits. The obtained REE budget is much higher, generally, comparable to the values quoted, for the Upper continental crust as reported by Rudnick and Gao (2010) (148 ppm). The REE budget of the bentonite study area shows intimate coherence (Fig. 36). The straightforward explanation of such discrepancies is that the REE content of the bentonite study area is strongly imparted by LREE signature.

7. Conflicts of interest

There are no conflicts to declare.

8. References

[1]Abayazeed, S.D., 2012, The Geochemistry of Some Egyptian Smectitic Clays. Australian Journal of Basic and Applied Sciences, 6(3), 589-599 pp.

[2]Abdel-Ghafour, N.G., El-Gammal, R.M. and Kamel, A., 1997, Mineralogical and facies composition of the Oligocene–early Miocene clay deposits, northern Western Desert, Egypt. 3rd Conf., II. Geochemistry Alexandria Univ., Egypt, pp. 161–168.

[3]Abdel-Motelib, A., Abdel-Kader, Z., Ragab, Y.A. and Mosalamy, M., 2011, Suitability of a Miocene Bentonite from North Western Desert of Egypt for Pharmaceutical Use, Applied Clay Science, PP.141.

[4]Abu El Ezz, A.R., Kholeif, M.M., and Abdo, A.A. (1993) Contribution to Mineralogy and Geochemistry of Some Bentonite Deposits in Egypt. El-Minia Science Bulletin, 6, 79-88.

[5]Agha, M.A., Ferrell, R.E., Hart, G.F., Abu El Ghar, M.S. and Abdel-Motelib, A. (2013) Mineralogy of Egyptian Bentonitic Clays II: Geologic Origin. *Clays and Clay Minerals*, **6**, 552-553.

[6]Ekosse, G. , 2001, *Provenance of the Kgwakgwe kaolin deposit in South Eastern Botswana and its possibile utilization.* Journal of applicable clay sciences. 20(3): 137-152.

[7]El-Nady, M.M. and Lotfi, N.M., 2015, *Multivariate geochemical and statistical methods applied to assessment of organic matter potentiality and its correlation with hydrocarbon maturity parameters (Case Study: Safir-1X well, NWD, Egypt)*, Egyptian Journal of Petroleum, pp.1-9.

[8]Faghihian, H. and Godazandeha, 2009, *Synthesis of Nano Crystalline Zeolite Y from Bentonite*, J Porous Material, pp.334-335.

[9]Fedo, C.M., Nesbitt, H.W. and Young, G.M, 1995, Unraveling the effects of potassium metasomatism in sedimentary rocks and paleosols, with implications for paleoweathering conditions and provenance. Geology 23, 921-924.

[10]Gromet L. P. and Dymek R. F., 1984, Nature and origin of orthopyroxene megacrysts from the St. Urbain anorthosite massif, Quebec. Can. Mineral. 22, 297-326.

[11]McLennan, S.M., 1989, Rare earth elements in sedimentary rocks: 1224influence of provenance and sedimentary processes. Rev. Mineral. 21, 169–200.

[12]Nesbitt, H.W. and Young, G.M, 1982, Early Proterozoic climates and plate motions inferred from major element chemistry of lutites. Nature, 199, 715-717.

[13]Rudnick, R.L. and Gao, S., 2010, Composition of the Continental Crust. In: Treatise on

Geochemistry. Holland, H.D. and Turekian, K.K. (Editors), Elsevier, Amsterdam. 3: 1-64.

[14]Shaban, M., Abukhadra, M. R., Shahien, M.G., Suzan, S.I., 2017, Novel Bentonite/Zeolite-NaP Composite Efficiently Removes Methylene Blue and Congo Red Dyes. Environ Chem. Lett. Springer International Publishing. DOI 10.1007/s10311-017-0658-7.

[15]Tawadros, E. (2001) A.A. Balkema, Rotterdam, The Netherlands. *Geology of Egypt and Libya*, 468 pp.

[16]Welton, J.E., 1984, SEM Petrology Atlas. AAPG Methods in Exploration Series, **4,** 237 pp, Tulsa.

[17]Weyer, S., Münker, C., Rehkämper, M. and Mezger, K., 2002, Determination of ultra-low Nb, Ta, Zr and Hf concentrations and the chondritic Zr/Hf and Nb/Ta ratios by isotope dilution analyses with multiple collector ICP-MS. Chem. Geol. 187, 295–313.

[18]Yousf, A.F., El Fakharany, M.A., Abu Risha, U.A., Afifi, M.M. and Al Sayyad, M.A., 2018, *Contributions to the Geology of Moghra-Qattara area, North Western*